# High Mobility Ge-Channel Formation By Localized/Selective Liquid Phase Epitaxy (LPE) Using Ge+B Plasma Ion Implantation And Laser Melt Annealing

John Borland[1], Shu Qin[2], Peter Oesterlin[3], Karim Huet[4], Walt Johnson[5], Lauren Klein[6], Gary Goodman[6], Alan Wan[6], Steven Novak[7], Thomas Murray[7], Richard Matyi[7], Abhijeet Joshi[8] and Si Prussin[8]

[1]J.O.B. Technologies, Aiea, Hawaii; [2]Micron Technology, Boise, Idaho; [3]Innovavent, Gottingen, Germany; [4]Excico, Paris, France; [5]KLA-Tencor, Milpitas, California; [6]EAG, East Windsor, New Jersey; [7]CNSE, Albany, New York; [8]UCLA, Los Angles, California
E-mail: JohnOBorland@aol.com

## 1. Introduction

Localized Ge and SiGe high mobility channel material is needed for 10nm node and beyond CMOS technology. Thin direct >50% SiGe selective epi followed by oxidation for Ge condensation, 100% Ge selective epi or thermal mixing are methods that require a hard mask and epi interface defects with rough surfaces are always an issue. An alternative approach to epi is using photoresist masking as proposed by Borland et al [1] with Ge-infusion doping (dose controlled deposition), a very high dose implantation technique that leads to amorphous deposition followed by low temperature SPE of the amorphous Ge surface layer but residual interface defects remained.

Today, laser melt annealing of implanted junctions with <300nm melt depths using 308nm and 515nm wavelength laser annealing equipment are currently being used in production for high quality back-side CMOS image sensor used in smart phone cameras by several IC and foundry semiconductor manufacturers to completely eliminate any residual implant damage/defects with 100% dopant activation provided the melt depth exceeds the implant damage depth [2]. In the solar industry selective emitter junction formation by laser melt annealing (LMA) is also used in production for high efficiency c-Si and mc-Si solar cells achieving 100% dopant electrical activation [3,4]. Aid et al [5] also reported shallow silicon surface melting at lower temperatures for an amorphous-Si surface at 1147°C formed by Ge-PAI + B implantation. Therefore in this paper we investigated another alternative approach combining very high dose Ge+B-plasma implantation and selective surface laser melt annealing (c-Si at 1407°C, a-Si at 1147°C, 50% c-SiGe at 1075°C and c-Ge at 937°C) using short wavelength 308nm and 515nm nsec laser annealing techniques with Si absorption depth of <7nm and <1000nm respectively.

## 2. Experimentation

N-type 300mm wafers were plasma implanted 1st with Ge and then B as listed in Table I. The $GeH_4$ energy was 3kV and $B_2H_6$ energy was 500V to achieve shallow Ge amorphous layer <10nm and B ultra-shallow junction <10nm. The plasma implant times for Ge & B are also shown in Table I varying from 4.5sec for $4E15/cm^2$ dose up to 66sec for $1E17/cm^2$ dose.

| Slot # | 1st PLAD Recipe | Implant Time (sec) | 2nd PLAD Recipe | 2nd Implant Time (sec) | Anneal |
|---|---|---|---|---|---|
| 13 | GEH3K1E16 | 8.6 | + BH500V4E15 | 4.5 | Laser-Innovavent |
| 14 | GEH3K1E16 | 8.6 | + BH500V4E15 | 4.4 | Laser-Excico |
| 15 | GEH3K1E17 | 66.0 | + BH500V4E15 | 4.4 | Laser-Innovavent |
| 16 | GEH3K1E17 | 66.0 | + BH500V4E15 | 4.4 | Laser-Excico |
| 17 | GEH3K1E17 | 66.0 | + BH500V4E16 | 42.5 | Laser-Innovavent |
| 18 | GEH3K1E17 | 66.0 | + BH500V4E16 | 42.5 | Laser-Excico |
| 19 | NA | NA | BH500V4E15 | 4.5 | Laser-Innovavent |
| 20 | NA | NA | BH500V4E15 | 4.5 | Laser-Excico |
| 21 | NA | NA | BH500V4E16 | 42.5 | Laser-Innovavent |
| 22 | NA | NA | BH500V4E16 | 42.5 | Laser-Excico |

Table I: Plasma implant conditions.

XPS analysis of the Ge-plasma implanted wafers just after implant was performed and shown in Fig.1. The results for the 3kV Ge $1E17/cm^2$ implant show that the Ge peak concentration is 55% while the $1E16/cm^2$ Ge wafer had a Ge peak concentration of 20%.

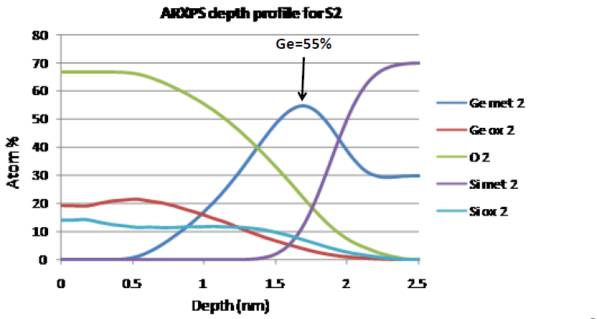


Fig.1: XPS depth profile analysis for the 3kV Ge $1E17/cm^2$ plasma implantation.

After implant the wafers were laser melt annealed using two different wavelength lasers. A 308nm UV laser with power levels from 0.2 $J/cm^2$ up to 3.0 $J/cm^2$ with a square step and repeat annealing pattern shown in Fig.2 and a 515nm green laser with power level variation from 0.25 $J/cm^2$ to 5.0 $J/cm^2$ with line-stripe annealing pattern shown in Fig.3.

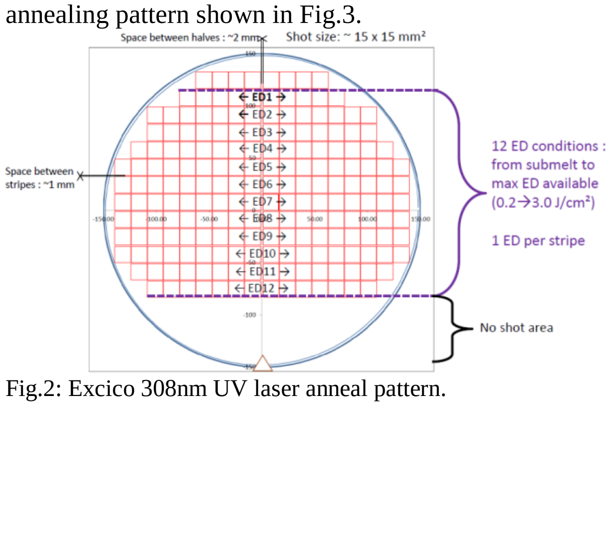


Fig.2: Excico 308nm UV laser anneal pattern.

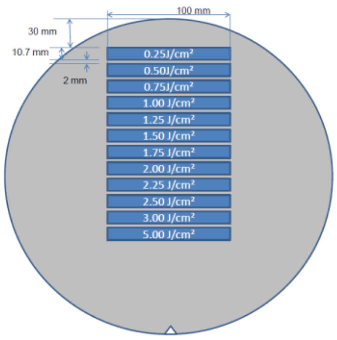


Fig.3: Innovavent 515nm green laser anneal pattern.

## 3. Results

*308nm UV Laser*

Residual implant damage recovery after laser melt annealing was monitored by therma-wave (TW) analysis as shown in Fig.4. For the 55% Ge wafer the melt threshold with the 308nm laser was ~0.35 J/cm$^2$ with complete damage recovery at 2.5 J/cm$^2$ for the BH=4E15/cm$^2$ case and 2.0J/cm$^2$ for the BH=4E16/cm$^2$ case. For the 20% Ge wafer the melt threshold was ~1.1 J/cm$^2$ with complete damage recovery by 1.5 J/cm$^2$.

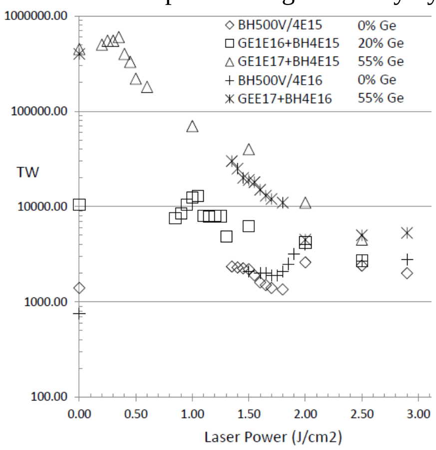


Fig.4: TW implant damage anneal.

Sheet resistance (Rs) measurements using special Hx-probe 4PP system are shown in Fig.5. For the 55% Ge wafers the B dopant activation threshold with the 308nm laser is at 0.35 J/cm$^2$ consistent with the TW results in Fig.4 but the Rs value was extremely high at >1 Mega Ω/□ reducing to 6K Ω/□ at 1.0J/cm$^2$ and then to the saturated level of 1K Ω/□ at 2.5J/cm$^2$. For the 20% Ge wafer the activation threshold is at 1.10J/cm$^2$, a shift of +0.75J/cm$^2$ clearly demonstrating our proposed selective/localized laser melt annealing approach however again the Rs value is high at ~25,000 Ω/□ and drops to a saturated value of 500 Ω/□ at 2.5 J/cm$^2$. In comparison the 0% Ge wafer Rs values drop to below 300 Ω/□ by 2.0 J/cm$^2$ and increasing the BH to 4E16/cm$^2$ reduces Rs to <100 Ω/□ however, adding Ge=1E17/cm$^2$ increases Rs to >300 Ω/□. From reported Rs versus implant dose with laser melt annealing the estimated electrical active dopant level can be extracted in Fig.6 [3, 4]. For 0% Ge the melt retained B concentration for BH=4E16/cm$^2$ is ~1E15/cm$^2$ (2.5%) and for BH=4E15/cm$^2$ is ~4E14/cm$^2$ (10%). With 20% Ge and BH=4E15/cm$^2$ the melt retained B concentration is ~2E14/cm$^2$ (5%) and with 55% Ge, B is ~9E13/cm$^2$ (2%). These retained $B_2H_6$ concentration values are much lower than for $BF_3$ also shown in Fig.6 [4].

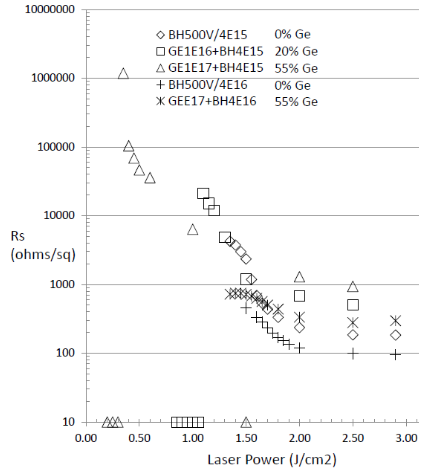


Fig.5: Rs dopant activation.

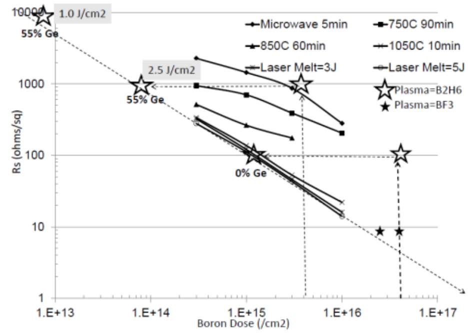


Fig.6: Rs versus B dose and Ge% for LMA [3, 4].

Ge, B, O and C SIMS depth analysis of the 308nm laser melt annealed wafers are shown in Fig.7 for 1.0J/cm$^2$. The melt depth is ~35nm with a Ge surface level of 60%, B~3E19/cm$^3$, O~5E20/cm$^3$ and C~2E20/cm$^3$. Fig.8 shows the results for the 2.5 J/cm$^2$ with a melt depth of ~160nm, graded Ge concentration ~5-25%, B~8E18/cm$^3$, O~2-5E18/cm$^3$ and C~1-3E19/cm$^3$. Note that O level drops by 100x and C by 10x for the deeper Si-melt depth.

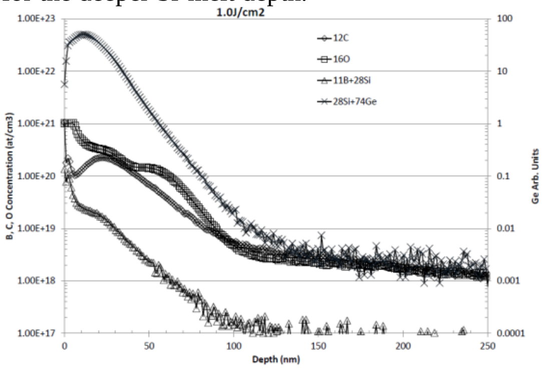


Fig.7: SIMS analysis at 1.0J/cm$^2$ for 55% Ge.

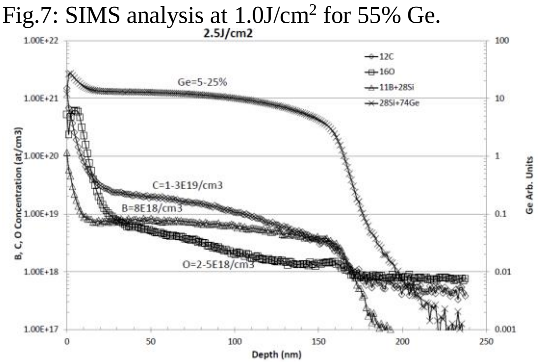


Fig.8: SIMS analysis at 2.5 J/cm$^2$ for 55% Ge.

Differential hall analysis was used for mobility and carrier depth profiles. The 0% Ge mobility reference value is 38cm$^2$/Vs and as shown in Fig.9, 20% Ge wafer increases hole mobility by 70% up to 63cm$^2$/Vs while the 55% Ge wafer near surface mobility (<5nm) increases up to 160cm$^2$/Vs or 4.3x higher surface hole mobility equivalent to 75% Ge or 1.5GPa of compressive strain-Si. Since the Ge-SIMS surface peak is ~25% the hole mobility should be ~80cm$^2$/Vs so the additional gain in mobility of 2x must be from additional surface Ge strain (see X-TEM).

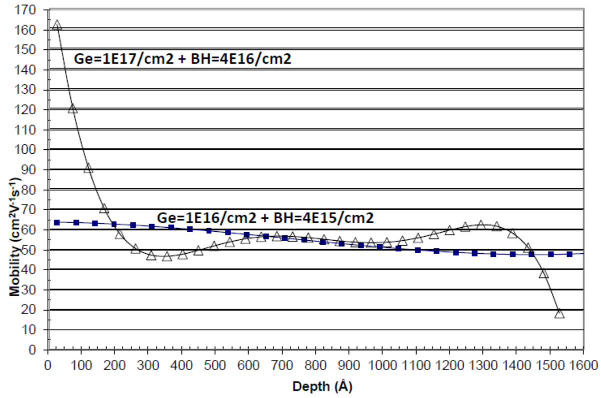


Fig.9: Mobility depth profiles.

The carrier depth profiles are shown in Fig.10 and Rs depth profiles in Fig.11. The BH=4E15/cm$^2$ has a B dopant level in the melt of ~8E18/cm$^3$ similar to the B-SIMS level in Fig.8 and a surface Rs value of ~530Ω/□ in Fig.11 in agreement with Rs in Fig.5. The BH=4E16/cm$^2$ wafer has B~1.2E19/cm$^3$ in Fig.10 with surface Rs~300Ω/□ in Fig.11 again good agreement with Fig.5.

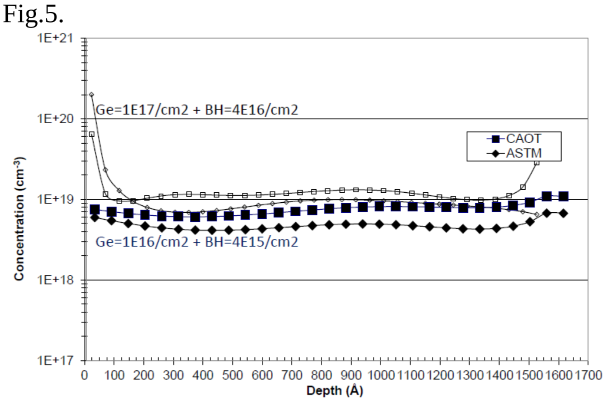


Fig.10: Carrier depth profiles.

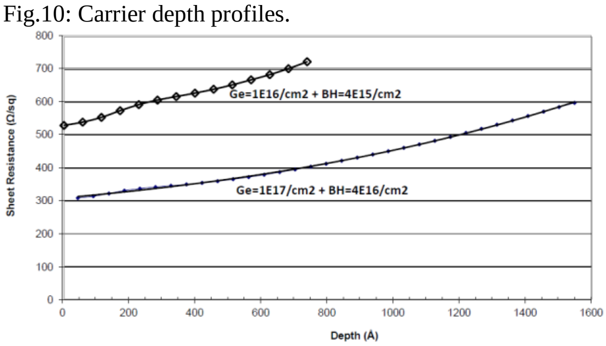


Fig.11: Sheet resistance depth profiles.

XRD strain-Si analysis is shown in Fig.12. Only the 55% Ge wafer with 2.5J/cm$^2$ anneal showed a slight shift in the XRD analysis and not representative of the 4x increase in hole mobility in the top 5nm as shown in Fig.9.

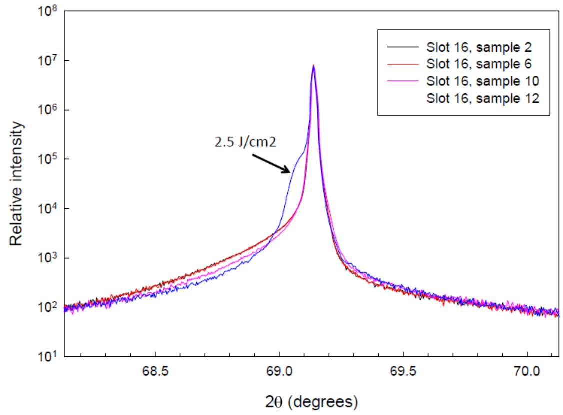


Fig.12: XRD strain-Si analysis for the 55% Ge wafer.

X-TEM results for the 55% Ge wafer are shown in Fig.13. Note the unannealed 0.0J/cm$^2$ shows a surface amorphous-SiGe (a-SiGe) layer ~40nm with end-of-range (EOR) damage extending to ~70nm. The 1.0J/cm$^2$ melt depth is ~35nm leaving a rough poly-SiGe surface ~25nm with a 10nm mixture of amorphous & crystalline SiGe then EOR damage to ~70nm. However, the 2.5J/cm$^2$ melt depth of ~160nm results in defect free LPE c-SiGe top surface region with a dark surface band ~5nm of strained-SiGe.

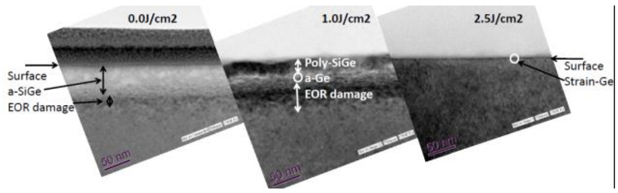


Fig.13: X-TEM analysis of Ge=55% wafer.

A plot of Si-melt depth based on SIMS analysis versus laser power level and Ge concentration is shown in Fig.14 for the 308nm UV laser clearly showing selective and deeper melt depth for the 55% Ge concentration wafer especially at lower power levels but converge at higher power levels.

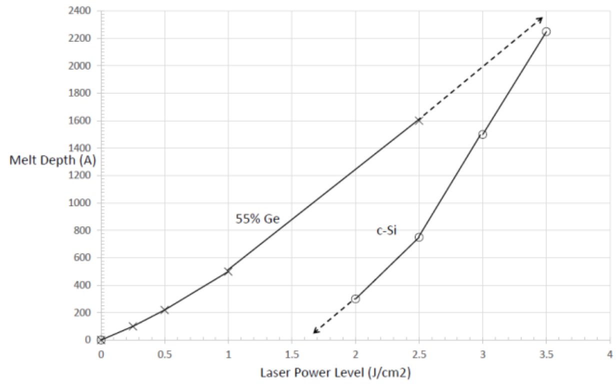


Fig.14: Si-melt depth versus laser power and Ge %.

*515nm Green Laser*

TW analysis for implant damage recovery for the 515nm LMA is shown in Fig.15. For the 55% Ge wafer the melt threshold is at >0.5J/cm$^2$ while the 20% Ge is at >1.0J/cm$^2$. The 3 wafers with 0% Ge varied in melt threshold from 0.75 to 1.25J/cm$^2$ so surface melt selectivity could not be clearly defined. This was also seen in the 4PP-Rs analysis of dopant activation shown in Fig.16. >1.0 J/cm$^2$ was the threshold for both the 55% and 0% Ge wafers with BH=4E15/cm$^2$ however, for the 20% and other 0% Ge wafers the threshold was

>1.25J/cm$^2$. Adding Ge also increased Rs by 3x from 150Ω/□ to 400Ω/□.

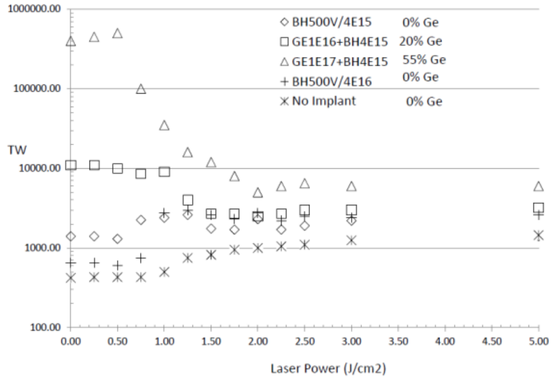


Fig.15: TW defect analysis.

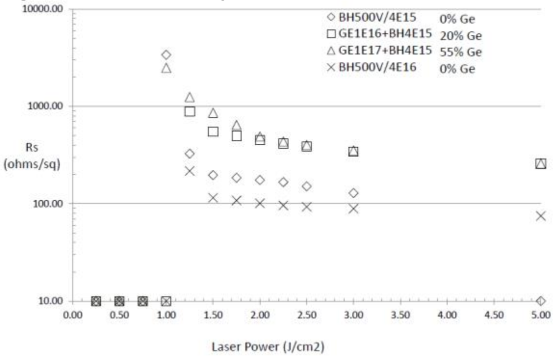


Fig.16: Rs-4PP analysis.

Ge & B SIMS depth profile analysis on the 3kV Ge 1E17/cm$^2$ + BH500V 4E15/cm$^2$ wafer with 515nm green laser LMA are shown in Figs. 17 & 18. The unannealed case shows a Ge surface concentration level of 55% ~3nm in agreement with XPS in Fig.1. The 0.5J/cm$^2$ LMA Ge liquid phase diffusion (melt) was ~10nm deep with a Ge surface concentration of ~45% and the 1.0J/cm$^2$ LMA melt depth was ~22nm resulting in a graded Ge surface profile from 10% to 40%. With 2.0J/cm$^2$ LMA the Ge melt depth was ~95nm with a graded Ge profile from 2% to 30%.

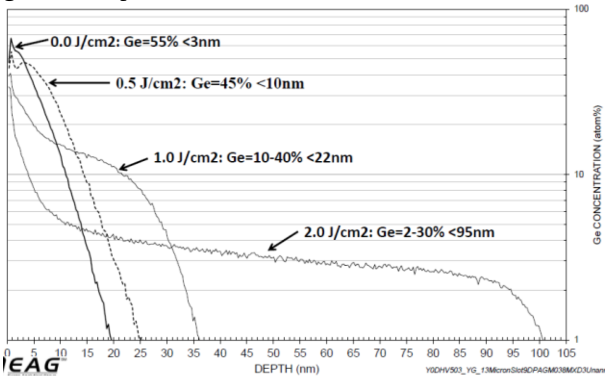


Fig.17: Ge-SIMS analysis with 515nm laser.

The B-SIMS profiles are shown in Fig.18. The unannealed B profile Xj was ~10nm with a very low retained dose of only 4.1E14/cm$^2$ (10%). Only a slight change in the B profile occurred with the 0.5 J/cm$^2$ LMA where the surface peak B level drops from 2E21/cm$^3$ to <8E20/cm$^3$ with no evidence of B surface box-like melt profile and B retained dose was 2.2E14/cm$^2$. With 1.0J/cm$^2$ the B liquid phase diffusion level was ~7E19/cm$^3$, melt depth ~20nm and B retained dose of 2.4E14/cm$^2$. The 2.0J/cm$^2$ LMA B melt depth was ~95nm with a B melt box-profile level of 2-3E19/cm$^3$ and retained B dose of 3.3E14/cm$^2$. Fig.19 shows the Si-melt depth versus Ge % and laser power and the trends are opposite to Fig.14. For the 515nm green laser at lower power levels they converge while at higher power 55% Ge melt depth is much shallower than 0% Ge. May need longer pulse duration.

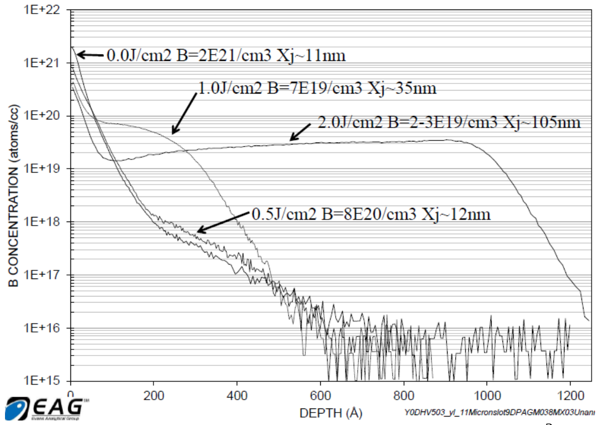


Fig.18: B-SIMS analysis at 0, 0.5, 1.0 and 2.0 J/cm$^2$ with 515nm laser.

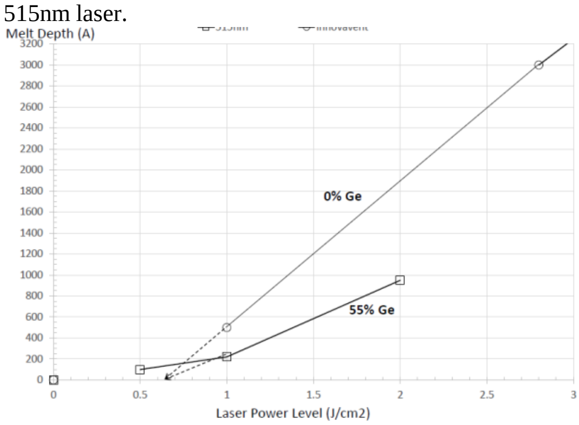


Fig.19: Si-melt depth versus Ge % for 515nm laser.

## 4. Summary


Our results show that with a 308nm laser we could achieve shallow melt threshold selectivity for 55% a-Ge at much lower power levels (0.35J/cm$^2$) than for 0% Ge (>1.3J/cm$^2$). With a 515nm laser the opposite was observed. Differential hall analysis showed the 55% Ge wafer surface mobility increased by 4.3x from 37 to 160 cm$^2$/Vs equivalent to 1.5 GPa of strain.



**Acknowledgements**

The authors would like to acknowledge Micron for providing the Ge+B plasma implantations and XPS analysis. Excico in France provided the 308nm LMA while Innovavent in Germany provided the 515nm LMA. KLA-Tencor in Shanghai, China provided the TW and Hx-4PP measurements. CNSE (College of Nanoscale Science and Engineering) in Albany, New York provided SIMS, XRD and X-TEM analysis. EAG in New Jersey also provided PICOR-SIMS analysis. UCLA in Los Angles provided differential hall measurements for hole-mobility and carrier depth profiles.


**References**


[1] J. Borland et al., ECS Oct 2004 meeting, PV 2004-07, p.769.
[2] S. Wuu et al., IEDM-2010, paper 14.1.
[3] J. Borland et al., IEEE-Photovoltaic Specialist Conference, June 2012, paper 626-J6.
[4] J. Borland et al., EU-PVSEC-2012, paper 2AV.6.34.
[5] S. Aid et al., IWJT-2010, paper S9-4.